 doi:10.20944/preprints202104.0079.v1

Article

CdTe X/γ-ray detectors with different contact materials

Volodymyr Gnatyuk [1,*], Olena Maslyanchuk [2,*], Mykhailo Solovan [2], Viktor Brus [3] and Toru Aoki [4]

[1] V.E. Lashkaryov Institute of Semiconductor Physics of the National Academy of Sciences of Ukraine, Prospekt Nauky 41, Kyiv 03028, Ukraine; gnatyuk@ua.fm
[2] Yuriy Fedkovych Chernivtsi National University, Kotsyubynskyi Str. 2, Chernivtsi 58012, Ukraine; emaslyanchuk@yahoo.com (O.M.); m.solovan@chnu.edu.ua (M.S.)
[3] Nazarbayev University, Nur-Sultan 010000, Republic of Kazakhstan; viktor.brus@nu.edu.kz
[4] Research Institute of Electronics, Shizuoka University, Johoku, Hamamatsu 432 8011, Japan; aoki.toru@shizuoka.ac.jp
* Correspondence: gnatyuk@ua.fm (V.G.); emaslyanchuk@yahoo.com (O.M); Tel.: +380-44-525-6040 (V.G.); +380-37-255-0244 (O.M.)

Abstract: Different contact materials along with optimization of the deposition techniques expand the possibilities to obtain high performance room temperature CdTe-based X/γ-ray detectors. The heterostructures with ohmic (MoO_x) and Schottky (MoO_x, TiO_x, TiN, and In) contacts, created by DC reactive magnetron sputtering and vacuum thermal evaporation, as well as In/CdTe/Au diodes with a *p-n* junction, formed by laser-induced doping, were developed and investigated. Depending on the pre-treatment of the surface of semi-insulating *p*-CdTe crystals, deposition of a MoO_x film formed an ohmic or Schottky contact. Based on the calculations and *I-V* characteristics of the fabricated Mo-MoO_x/*p*-CdTe/MoO_x-Mo, In/CdTe/MoO_x-Mo, Ti-TiO_x/*p*-CdTe/MoO_x-Mo, and Ti-TiN/*p*-CdTe/MoO_x-Mo Schottky-diode detectors, the current transport processes were described in the models of the carrier generation-recombination within the space-charge region (SCR) at low bias voltages, and space-charge limited current at higher voltages, respectively. The energies of generation–recombination centers, density of trapping centers, and carrier lifetimes were determined. A sharp increase in the reverse current in the Mo-MoO_x/*p*-CdTe/MoO_x-Mo, Ti-TiO_x/*p*-CdTe/MoO_x-Mo, and Ti-TiN/*p*-CdTe/MoO_x-Mo heterostructures at high bias was discussed in frames of the Poole–Frenkel emission model. Nanosecond laser irradiation of the In electrode, pre-deposited on the *p*-CdTe crystals, resulted in an increase in the voltage range, corresponding to the carrier generation-recombination in the SCR, in the *I-V* characteristics of the In/CdTe/Au diodes. Such In/CdTe/Au *p-n* junction diodes demonstrated high energy resolutions (7%@59.5 keV, 4%@122 keV, and 1.6%@662 keV).

Keywords: CdTe detectors; X-ray and gamma ray spectroscopy; Schottky contact; *p-n* junction; charge transport mechanism

1. Introduction

One of the key properties of semiconductors, known as the photo-effect, makes these materials the best candidates for photo-sensors for a wide spectral range (from γ-rays to terahertz radiation). Indeed, thanks to the great ability to directly convert photons to electric charge carriers, i.e. an electrical signal, semiconductor detectors have significant advantages compared with other ionizing radiation sensors such as scintillators, gas-based detectors, etc. [1]. The favorable features of semiconductor nuclear radiation detectors are higher energy and spatial resolution, sufficient detection efficiency, rate and timing characteristics, enhanced imaging capabilities, and promising ability to fabricate compact sensor modules and portable detecting instruments [1,2].

Among many suitable semiconductors used for X/γ-ray (in other words, high-energy, nuclear, or ionizing radiation) detectors, cadmium telluride (CdTe) is the most studied, employed, and attractive compound because of its favorable physical properties [2-6]. Indeed, an optimal set of electrical and electronic characteristics of

Preprints (www.preprints.org) | NOT PEER-REVIEWED | Posted: 2 April 2021 doi:10.20944/preprints202104.0079.v1

high-resistivity CdTe makes this material basic and still promising for compact uncooled X/γ-ray detectors covering a wide energy range from a few keV to tens MeV, which are widely used in science, industry, security, ecology, medicine, space astronomy and many other application fields [3-8]. Among the excellent features of this semiconductor, there are key advantages that have to be highlighted: large atomic numbers of the compound components (Z_{Cd} = 48 and Z_{Te} = 52) provide high absorption efficiency of X/γ-photons, stopping power and therefore, high radiation attenuation coefficient; wide band-gap energy (E_g ~ 1.46 eV) and hence, quite high electrical resistivity ($\rho > 10^9$ Ω·cm) along with appropriate charge transport properties allow CdTe-based detectors to operate without liquid nitrogen or Peltier cooling [3-10]. As a result, uncooled CdTe-based detectors make it possible to achieve high radiation detection efficiency, energy resolution, and fast timing response to be efficiency employed for portable detecting devices [5-10].

High-resistivity CdTe single crystals have been successfully used in the fabrication of room temperature X/γ-ray detectors in two principally different ways (basic technologies): (i) by the creation of both ohmic electrical contacts and (ii) formation of a diode structure either with a Schottky contact or *p-n* junction [3-10]. CdTe detectors with two ohmic contacts operate at low bias voltage and have good time stability of the functional parameters (detection efficiency and energy resolution). However, ohmic contact detectors biased with low (tens volts) voltage suffer from an incomplete collection of radiation-generated carriers and hence, the considerable amount of charge losses because holes can be trapped before reaching the cathode. Therefore, the energy resolution of ohmic detectors is not high enough but higher bias voltage (hundreds of volts) cannot be applied because of an increase in leakage (dark) current [5-10].

Diode-type detectors operating in a reverse mode reduce leakage current that makes it possible to increase bias voltage (up to thousand volts and higher) extend the depletion region, improve the charge collection and hence, increase energy resolution and detection efficiency [5-10]. The possibilities of creating CdTe-based X/γ-ray detectors with barrier structures have been shown since the 1960s [3,11]. However, CdTe diode-type detectors suffer from the charge polarization effect which is one of the important problems that deteriorate detector parameters with operation time and limits their application [3-8,12,13]. Therefore, both the basic techniques have recently been developed and used to fabricate ohmic and diode-type detectors [5-10].

Intensive and successful development of CdTe-based X/γ-ray detectors formed as Schottky diodes began at the end of 1990s when Acrorad Co. Ltd. obtained high quality (chemical purity, higher uniformity, structural perfection, reduced number of point and extended defects, etc.) bulk semi-insulating CdTe semiconductor and used a low work-function metal (indium) to create a high Schottky barrier for holes on the crystal surface that provided high energy resolution of In/CdTe/Pt diode X/γ-ray detectors [7-10]. Along with In, Al has been studied and employed as a Schottky contact to Acrorad's CdTe crystals [12,13]. Nowadays, Al/CdTe/Pt and In/CdTe/Pt Schottky diodes are generally used as main industrial high-resolution uncooled semiconductor X/γ-ray detectors [7-10, 12,13].

During the last 2 decades, we have widely used semi-insulating CdTe semiconductors, produced by Acrorad for material characterization [14,15] and elaboration of both Schottky diode-type [17-26] and M-*p-n* structured [26-33] X/γ-ray detectors. Using different metals (Ni, Cr, In, Al, and Au) for electrodes to form appropriate Schottky and ohmic electrical contacts or employing laser-induced doping of a thin CdTe layer with In, we have obtained high performance X/γ-ray diode-type detectors. In particular, we have achieved excellent energy resolution (FWHM of the 662 keV photopeak in the ^{137}Cs isotope spectra) at room temperature for Ni/CdTe/Ni Schottky diodes formed by Ar-ion bombardment (FWHM ~ 0.5%) [17-19,26] and for In/CdTe/Au detectors with a *p-n* junction created by laser induced doping (FWHM ~ 0.7-1.4%) [26,33].

We have recently studied other electrode materials (graphene, metal oxides and nitrides) different from metals used before and developed the techniques to employ them to form Schottky and ohmic electrical contacts to Acrorad's semi-insulating CdTe crystals

Preprints (www.preprints.org) | NOT PEER-REVIEWED | Posted: 2 April 2021 doi:10.20944/preprints202104.0079.v1

[20-25]. We have interested to develop this trend, in particular using molybdenum oxide as a promising material for ohmic contact formation [34-39]. In addition, titanium oxide, titanium nitride, and indium have been employed for the creation of Schottky contacts. We have also fabricated CdTe-based M-*p*-*n* structured diodes developing the laser solid-phase doping technique [32,33]. The aim of this paper is to review our experience in the creation and study of CdTe-based structures for X/γ-ray detectors using the same material, i.e. detector-grade *p*-like crystals produced by Acrorad [8-10].

2. Semiconductor Samples

To meet the requirements for the materials to fabricate room temperature X/γ-ray detectors, we have widely and successfully employed commercial detector-grade *p*-like CdTe semiconductor, produced by Acrorad Co., Ltd. [8-10]. Semi-insulating CdTe semiconductor has been obtained by the Traveling Heater Method (THM), which is known as an advanced and efficient technique to grow high-quality single crystals (chemical purity, higher uniformity, structural perfection, reduced number of extended defects as well as relatively low concentration of native point defects and accidental impurities, etc.) [4-10].

High-resistivity Cl-compensated CdTe crystals showed weak *p*-type conduction with room temperature resistivity $\rho = (2\text{-}4) \times 10^9$ Ω·cm that was close or even higher than the intrinsic value ($\rho_i \approx 4 \times 10^9$ Ω·cm). The estimated electron and hole densities were $n \approx 4.2 \times 10^4$ cm^{-3} and $p \approx 2.6 \times 10^7$ cm^{-3} [9,10]. It was shown that the employed CdTe could be considered as an almost intrinsic semiconductor with the bandgap $E_g = 1.47$ eV (at $T = 300$ K), effective masses of electrons $m_n = 0.11m_0$ and holes $m_p = 0.53m_0$, where m_0 is the free electron mass [14,15].

The grown CdTe ingots were sliced into (111) oriented single-crystal wafers. The (111) crystal surfaces of CdTe exhibit crystallographic polarity. Usually, the close packed plane terminated by Cd atoms is called the *A*-face, whereas that terminated by Te atoms is called the *B*-face [2-6]. Conventionally, many properties of polar surfaces (CdTe(111)*A* and CdTe(111)*B*) differ considerably. Parallelepiped-like (111) oriented CdTe samples with a surface area of 5 × 5 mm^2 and thickness of 0.5 mm or 0.75 mm, preliminary polished by the manufacturer, were used in our experiments, i.e. for fabrication of CdTe-based heterostructures, Schottky diodes and M-*p*-*n* structures with different electrical contacts which then were tested as X/γ-ray detectors. Prior to employing the technological procedures of modification of the surface states, formation of electrical contacts, and electrode deposition, CdTe single-crystal wafers were subjected to preliminary surface processing for removing surface contaminations and cleaning. The features of the surface treatments for each case have been described in the corresponding sections below.

3. Capabilities of CdTe-Based X/γ-Ray Detectors with MoO_x Ohmic Contacts

3.1. Fabrication of CdTe-Based Detectors with MoO_x Ohmic Contacts

3.1.1. Molybdenum Oxide as a Prospective Material for Ohmic Contact Formation

Molybdenum oxide (MoO_x) has been widely used as an interlayer for the fabrication of high performance electrical contacts to low resistance *p*-CdTe semiconductor [34-36], in particular as a material with large work functions [37-39]. Moreover, MoO_x is favorably distinguished by its high transparency for visible radiation and relatively low specific electrical resistivity. Due to these properties and high work function (5.2-6 eV) [36], MoO_x has been considered and studied as a promising candidate to form efficient electrical contacts to semi-insulating *p*-CdTe semiconductor crystals [20-24].

Before electrical contact formation and electrode deposition, the investigated CdTe crystals were subjected to preliminary polishing chemical etching in a solution $K_2Cr_2O_7$ + HNO_3 + H_2O during 20-30 s. For fabrication of Mo-MoO_x/*p*-CdTe/MoO_x-Mo X/γ-ray de-

Preprints (www.preprints.org) | NOT PEER-REVIEWED | Posted: 2 April 2021 doi:10.20944/preprints202104.0079.v1

tectors with ohmic contacts, MoO_x films were deposited on the preheated up to ~100 °C surface of the CdTe substrates in a universal vacuum system Leybold-Heraeus L560 by DC reactive magnetron sputtering of a pure molybdenum target in an argon-oxygen mixture atmosphere during ~300 s. Prior to the electrode deposition process, the vacuum chamber was evacuated to a residual pressure of 5 mPa and the *p*-CdTe substrate surface was subjected to relatively long-term bombardment by Ar ions (ion beam intensity was ~15 mA/cm^2 and processing time was ~600 s) to create a *p*+-layer, which increased the ohmic contact quality. The partial pressures of argon and oxygen in the vacuum chamber under the MoO_x film deposition were 240 mPa and 34 mPa, respectively. The magnetron power was ~120 W. After the MoO_x film deposition, the oxygen supply was closed and deposition of a pure molybdenum film was carried out during ~60 s. Thanks to the optimal relationship of the work functions of *p*-CdTe and MoO_x, and the created *p*+-layer with an increased concentration of uncompensated acceptors, the Mo-MoO_x/*p*-CdTe/MoO_x-Mo ohmic structures with a minimum potential barrier at the contacts were formed.

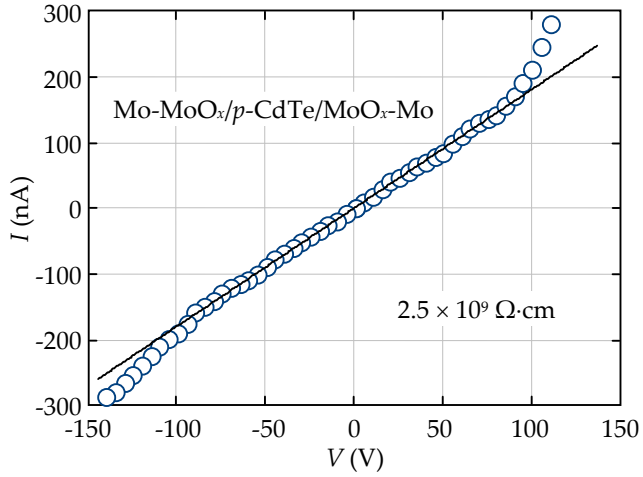

Figure 1. *I-V* characteristics of the Mo-MoO_x/*p*-CdTe/MoO_x-Mo detector with two ohmic contacts at both polarities of applied voltage (circles). The solid line demonstrates a linear voltage dependence of the current.

The fabricated Mo-MoO_x/*p*-CdTe/MoO_x-Mo ohmic detectors were characterized by electrical and spectroscopic measurements at room temperature. As seen from Figure 1, the *I-V* characteristic of the Mo-MoO_x/*p*-CdTe/MoO_x-Mo sample, measured with a delay time of 1.5 s, is symmetric and follows Ohm's law in the entire range of the applied bias voltage. Such a feature confirmed the formation of a high-quality ohmic contact at the MoO_x/*p*-CdTe interface. The slope of the voltage dependence of the current corresponds to a specific resistivity of 2.5 x 10^9 Ω·cm, which was the typical value for detector-grade high-resistivity CdTe material grown by Acrorad Co. Ltd. [8-10,15]. It should be noted, a sharper increase in the current is observed at $|V| > \pm 100$ V (Figure 1). This feature of the *I-V* characteristic, which manifests a non-ohmic behavior of the MoO_x/*p*-CdTe contacts, is discussed in detail in Section 3.2.

3.1.2. Schottky Contact Formation

Schottky and ohmic contacts were formed on the CdTe(111)*B* side (Te-terminated) and CdTe(111)*A* side (Cd-terminated) of crystals, respectively (Figure 2). The different conditions under Ar ion etching of the CdTe crystal surfaces were used before the electrode deposition and creation of Schottky and ohmic contacts. In particular, prior to the deposition of MoO_x, TiO_x, and TiN films, the *A*-face surface of the CdTe substrates was bombarded with Ar ions with the intensity of an ion beam about 5 mA/cm^2 (Figure 2b). The accelerating voltage was ~1000 V and the etching time was about 300 s. The distinctions between the properties of junctions (contacts) formed on the opposite sides of the CdTe(111) single-crystal wafers were attributed to the modification of the system of elec-

Preprints (www.preprints.org) | NOT PEER-REVIEWED | Posted: 2 April 2021 doi:10.20944/preprints202104.0079.v1

tronic states and the Fermi level pinning at the *A*-face (Cd-terminated) and *B*–face (Te-terminated) surfaces.

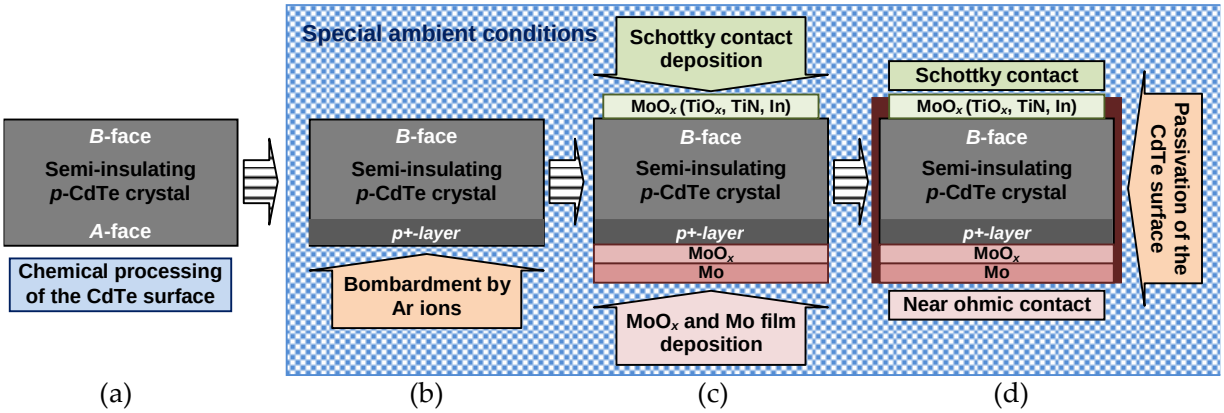

Figure 2. Schematic illustration of the fabrication procedures of $MoO_x(TiO_x$, TiN, In)/*p*-CdTe/MoO_x diode detectors: (**a**) chemical surface processing of the crystal; (**b**) bombardment by Ar ions to create a *p*+-layer on the CdTe(111)*A* surface; (**c**) Schottky (ohmic) contacts formation; (**d**) passivation of the crystal surfaces.

The MoO_x and TiO_x films were deposited by DC reactive magnetron sputtering of a molybdenum or titanium target at the CdTe substrate temperature ~100 °C in an argon-oxygen mixture atmosphere (partial pressures of argon and oxygen in the vacuum chamber were 240 mPa and 24 mPa, respectively) with the processing time of ~60 s (Figure 2c). Whereas a TiN thin film was deposited in an argon-nitrogen mixture atmosphere (partial pressures of argon and nitrogen were 350 mPa and 700 mPa, respectively) during ~15 min. Since the MoO_x, TiO_x, and TiN films deposited by DC reactive magnetron sputtering showed high electrical conductivity, we considered the MoO_x/*p*-CdTe, TiO_x/*p*-CdTe, and TiN/*p*-CdTe heterostructures as Schottky-type contacts. To form an In/*p*-CdTe Schottky contact, an In film was deposited by vacuum thermal evaporation of pure indium from a tungsten crucible. All the electrodes were circular with a diameter of 4 mm and were centered on the Te- and Cd-terminated surfaces of the CdTe(111) crystals (5 × 5 mm^2 squares), forming Schottky or ohmic contacts, respectively.

Afterward, the edges of the CdTe-based structures were coated with aluminum oxide (Al_2O_3) layer in order to passivate surface defects on the CdTe crystals, minimize undesirable surface and lateral leakage currents and protect the surface from degradation (Figure 2d). An Al_2O_3 thin film was deposited onto the formed CdTe structures by the DC reactive magnetron sputtering technique. Under the deposition process in an argon-oxygen mixture atmosphere, the partial pressures in the vacuum chamber were 400 mPa for both argon and oxygen. The magnetron power was ~150 W. The deposition process lasted for 10 min at the CdTe substrate temperature of ~100 °C.

3.2. Electrical Characteristics of CdTe-Based Detectors with MoO_x Ohmic Contacts

3.2.1. *I-V* Characteristics of CdTe-Based Heterostructures with MoO_x Contacts

The fabricated CdTe-based detectors with different Schottky contacts and MoO_x ohmic contacts were investigated by electrical measurements in the dark at different temperatures. Reverse currents in the CdTe diode structures flowed when the Schottky contact was biased positively with respect to the ohmic one. The *I-V* characteristics of the fabricated Mo-MoO_x/*p*-CdTe/MoO_x-Mo, Ti-TiO_x/*p*-CdTe/MoO_x-Mo, Ti-TiN/*p*-CdTe/MoO_x-Mo, and In/*p*-CdTe/MoO_x-Mo heterostructures showed rectification properties. In terms of the practical application of the developed CdTe-based structures for detection of X/γ-ray radiation, it is important to analyze the reverse branches of the *I-V* characteristics when the Schottky contact is biased positively with respect to the MoO_x-Mo ohmic contact because of diode-type detectors operate under reverse bias [4-8]. It should be noted that the reverse currents in the heterostructures under investigation are

Preprints (www.preprints.org) | NOT PEER-REVIEWED | Posted: 2 April 2021 doi:10.20944/preprints202104.0079.v1

equal to several nanoamperes at bias voltages of ~50–100 V at room temperature (Figure 3). This feature makes them promising for application as ionizing radiation detectors for spectroscopic devices.

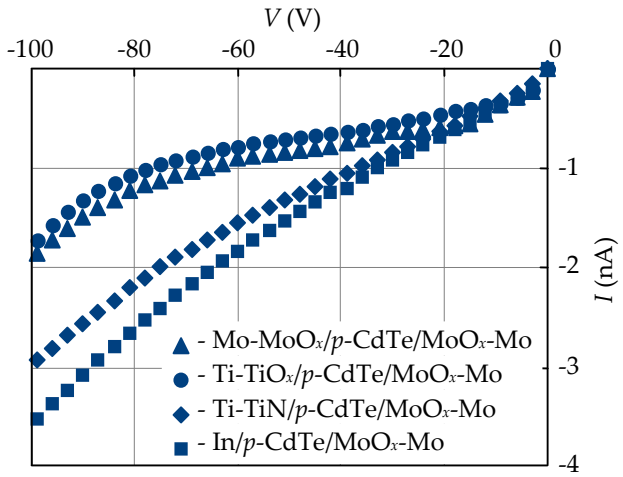

Figure 3. Reverse *I-V* characteristics of the CdTe-based Schottky-diode detectors with one MoO*x* contact and the second one made from different materials: MoO_x (triangles), TiO_x (circles), TiN (diamond), and In (squares).

The shape of the reverse *I-V* characteristics of the Mo-MoO_x/*p*-CdTe/MoO_x-Mo, Ti-TiO_x/*p*-CdTe/MoO_x-Mo, Ti-TiN/*p*-CdTe/MoO_x-Mo, and In/*p*-CdTe/MoO_x-Mo heterostructures, plotted in double logarithmic coordinates, clearly indicates the existence of some specific regions (Figure 4). As seen, the Mo-MoO_x/*p*-CdTe/MoO_x-Mo Schottky-diode detector (a) at the bias voltages $0.01 < V < 100$ V and In/*p*-CdTe/MoO_x-Mo Schottky-diode detector (b) at the bias voltages $0.01 < V < 60$ V demonstrate a square-root voltage dependence of the current, indicating the generation nature of charge transport (Figure 4). This is quite understandable, according to the Sah-Noyce-Shockley theory of generation-recombination of charge carriers in the space-charge region (SCR), because when the reverse bias voltage satisfies the condition $qV > kT$, the multiplier $[\exp(qV/2kT) - 1]$ does not play any role and thus the dependence $I(V)$ becomes square-root-like ($I \sim V^{1/2}$) [40,41]. Here, q is the electron charge and k is the Boltzmann constant.

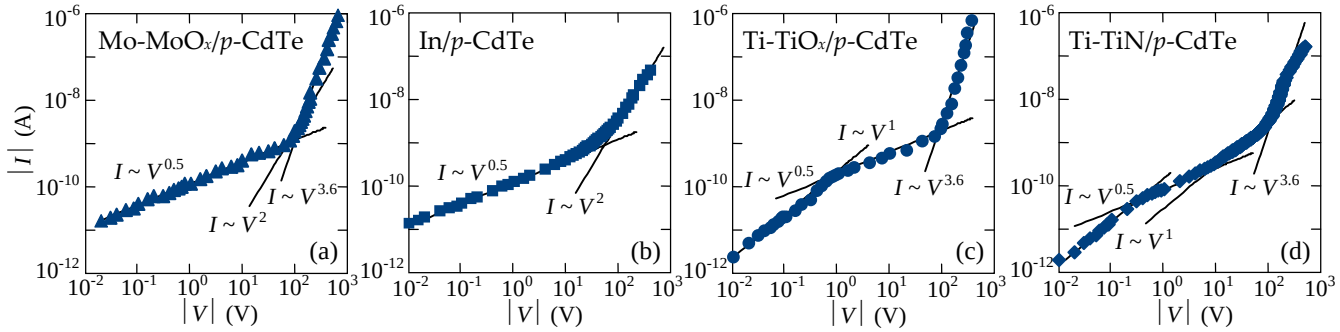

Figure 4. Reverse *I-V* characteristics of the (**a**) Mo-MoO_x/*p*-CdTe/MoO_x-Mo, (**b**) In/*p*-CdTe/MoO_x-Mo, (**c**) Ti-TiO_x/*p*-CdTe/MoO_x-Mo, and (**d**) Ti-TiN/*p*-CdTe/MoO_x-Mo Schottky-diode detectors in double logarithmic coordinates (symbols). Approximations of the square-root ($I \sim V^{0.5}$), linear ($I \sim V$), square-law ($I \sim V^2$), and power-law ($I \sim V^{3.6}$) voltage dependences of the current are shown by solid lines.

An additional confirmation of that assumption is provided by the comparison of the experimental *I-V* characteristics with the calculation results obtained in the frame of the Sah-Noyce-Shockley theory of generation-recombination of carriers, which was adapted to a metal-semiconductor (Schottky) contact (Figure 5). According to the theory [40], the

Preprints (www.preprints.org) | NOT PEER-REVIEWED | Posted: 2 April 2021 doi:10.20944/preprints202104.0079.v1

generation current I_g can found by integration of the generation rate $U(x)$ in the SCR throughout the entire SCR as shown in [16,20-24,41-44]

$$I_g = A\,q\int_0^W \frac{n(x,V)\,p(x,V)-n_i^2}{\tau_{p0}\left[n(x,V)+n_1\right]+\tau_{n0}\left[p(x,V)+p_1\right]}dx\,, \tag{1}$$

where A is the diode area, q is the electron charge, W is the width of the SCR, $n_i = (N_cN_v)^{1/2}\exp(-E_g/2kT)$ is the intrinsic carrier concentration ($N_c = 2(m_nkT/2\pi\hbar^2)^{3/2}$ and $N_v = 2(m_pkT/2\pi\hbar^2)^{3/2}$ are the effective state densities in the conduction and valence bands, respectively, then m_n and m_p are the effective masses of electrons and holes, respectively, τ_{p0} and τ_{n0} are the lifetimes of holes and electrons in the SCR, x is the coordinate where an electron–hole pair is generated. The values n_1 and p_1 are equal to the equilibrium concentrations of electrons and holes, respectively, under the condition that the Fermi level in the semiconductor coincides with the generation-recombination level with the ionization energy E_t (calculated from the top of the valence band). That is, $n_1 = N_c\exp(-E_t/kT)$ and $p_1 = N_v\exp[-(E_g-E_t)/kT]$. The values $n(x,V)$ and $p(x,V)$ are the concentrations of carriers in the conduction and valence band within the SCR, respectively

$$n(x,V) = N_c\exp\left[-\frac{E_g-\Delta\mu-\varphi(x,V)-qV}{kT}\right] \qquad p(x,V) = N_v\exp\left[-\frac{\Delta\mu+\varphi(x,V)}{kT}\right], \tag{2}$$

where $\Delta\mu$ is the energy location of the Fermi level in the semiconductor.

The potential energy $\varphi(x,V)$ of an electron in the SCR is described by the equation

$$\varphi(x,V) = (\varphi_0 - qV)\left(1-\frac{x}{W}\right)^2, \tag{3}$$

where φ_0 is the barrier height from the CdTe semiconductor side. The width of the SCR is expressed as [46]

$$W = \sqrt{\frac{2\varepsilon\varepsilon_0(\varphi_0-qV)}{q^2N}}\,, \tag{4}$$

where ε is the relative dielectric permittivity of the semiconductor, ε_0 is the dielectric constant of vacuum.

The calculation results at different temperatures are shown by the solid line in the I–V characteristics of the heterostructures (Figure 5). The ionization energy of the generation–recombination center E_t was chosen to be equal to 0.69-0.70 eV, i.e., when the energy level of the center was located near the middle of the semiconductor bandgap (E_g = 1.47 eV at room temperature), as it was described by the Shockley–Read–Hall statistics [16,46].

The width of the SCR (Equation (4)) was calculated at the concentration of uncompensated acceptors $N = N_a - N_d = 5\times10^{10}$ cm^{-3} like in CdTe single crystals produced by Acrorad [19-25]. The temperature dependences of the bandgap $E_g(T) = 1.608 - 4.52\times10^{-4}\times T$ (eV), holes mobility $\mu_p = 4\times10^5\times T^{3/2}$ (cm^2/V·s), and resistivity of CdTe were taken into account [14,15,19]. To ensure the best coincidence of the experimental data with the calculation results, the lifetime of electrons and holes in the SCR were chosen to be equal to $\tau_{n0} = \tau_{p0} = 2.0\times10^{-7}$ s. The voltage range in the calculations for every detector was used where square-root voltage dependences of the current were fulfilled (Figure 4).

Preprints (www.preprints.org) | NOT PEER-REVIEWED | Posted: 2 April 2021 doi:10.20944/preprints202104.0079.v1

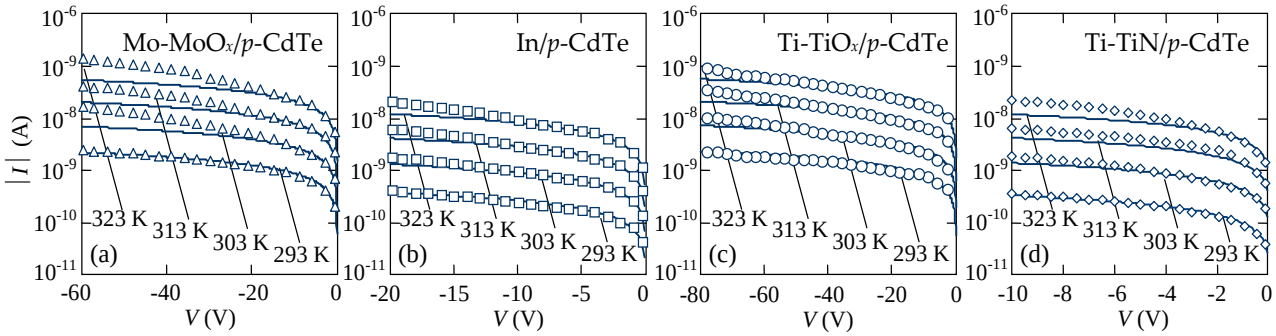

Figure 5. Comparison of the experimental (symbols) and calculated according to the Sah-Noyce-Shockley theory (solid lines) results of the reverse *I-V* characteristics of the (**a**) Mo-MoO$_x$/*p*-CdTe/MoO$_x$-Mo, (**b**) In/*p*-CdTe/MoO$_x$-Mo, (**c**) Ti-TiO$_x$/*p*-CdTe/MoO$_x$-Mo, and (**d**) Ti-TiN/*p*-CdTe/MoO$_x$-Mo Schottky-diode detectors at different temperatures.

Another feature of the diodes under study is the fact that the magnitude of the generation current I_g is proportional to the concentration of intrinsic charge carriers in the semiconductor, i.e. the activation energy, which is determined from the slope of the dependence $\log(I_g/T^{3/2})$ versus $10^3/T$, equals 0.8 eV that corresponds to the half of the CdTe bandgap at 0 K [22,24]. Therefore, a very good agreement between the measurement and calculation results is observed confirming that the model of the generation-recombination processes in the SCR adequately describes not only the voltage dependences of the current, but also the temperature-induced variations in the *I–V* characteristics of the CdTe-based detectors with different contact materials [20-24].

For the fabricated Ti-TiO$_x$/*p*-CdTe/MoO$_x$-Mo and Ti-TiN/*p*-CdTe/MoO$_x$-Mo heterostructures, the generation nature of the reverse current is also observed in the voltage range 0.6 V< V < 90 V and 0.3 V < V < 15 V, respectively (Figure 4c,d). A good agreement of the experimental and calculated results confirms this assumption (Figure 5c,d). However, quite long initial linear region ($I \sim V^1$) of the reverse *I–V* characteristics precedes the square-root region in the dependence $I(V)$ (Figure 4c,d). This can be explained by the fact that the barrier height at the TiO$_x$/*p*-CdTe and TiN/*p*-CdTe contacts (φ_0 = 0.3 eV) is lower than that at the MoO$_x$/*p*-CdTe and In/*p*-CdTe ones (φ_0 = 0.6 eV). According to Equation (4), the depleted region in the TiO$_x$/*p*-CdTe and TiN/*p*-CdTe diode structures is thinner than in the MoO$_x$/*p*-CdTe and In/*p*-CdTe ones, and thus its resistance is smaller. This circumstance explains the fact that the reverse current flowed through the MoO$_x$/*p*-CdTe and In/*p*-CdTe diode structures at low bias voltages is controlled by the reverse-biased Schottky contact, whereas the initial linear region of the reverse *I–V* characteristic of the TiO$_x$/*p*-CdTe and TiN/*p*-CdTe diode structures is attributed to the fact that the resistance of the neutral (bulk) part of the CdTe crystal is comparable or even higher than the resistance of the depletion region at low reverse bias. Therefore, the CdTe crystal bulk (neutral part) controls the reverse current in the initial region of the *I-V* characteristic of the Ti-TiO$_x$/*p*-CdTe/MoO$_x$-Mo and Ti-TiN/*p*-CdTe/MoO$_x$-Mo Schottky-diode detectors [20-24].

3.2.2. Features of CdTe-Based Heterostructures with MoO$_x$ Contacts at Higher Bias

However, a further increase in reverse bias ($|V|$ > 100 V), applied to the Mo-MoO$_x$/*p*-CdTe/MoO$_x$-Mo and In/*p*-CdTe/MoO$_x$-Mo heterostructures changes the current transport mechanism. The *I–V* characteristics become proportional to the squared voltage ($I \sim V^2$) (Figure 4a,b), i.e. the Mott-Gurney law for the space-charge-limited current (SCLC) is fulfilled. This is typical for semi-insulating materials [47,48]. Thus, the SCLC is expressed by the equation

$$I_{\mathrm{SCLC}} = \theta \cdot \frac{9}{8}\frac{\varepsilon\varepsilon_0\mu}{d^3}V^2 = \frac{N_{\mathrm{v}}}{N_{\mathrm{t}}}\exp\left(-\frac{E_{\mathrm{t}}}{kT}\right)\frac{9}{8}\frac{\varepsilon\varepsilon_0\mu}{d^3}V^2, \quad (5)$$

Preprints (www.preprints.org) | NOT PEER-REVIEWED | Posted: 2 April 2021 doi:10.20944/preprints202104.0079.v1

where μ is the mobility of charge carriers, d is the distance between the electrodes, i.e. the semiconductor crystal thickness. The factor θ takes into account the presence of accident impurities and point defects (traps), creating deep levels in the bandgap of a semiconductor. Such deep-level traps are inherent in CdTe because some number of uncontrolled impurities and corresponding intrinsic defects are always present in the semiconductor.

Discussing the nature of excess concentration of charge carriers (necessary for space-charge-limited transport) in the Schottky-diode detectors under study, it is likely to explain the observed rapid increase in the current by the imperfection of the CdTe/MoO_x ohmic contact. Then, if even a small downward band bending φ_2 exists (Figure 6a), the CdTe/MoO_x contact becomes forward-biased. Consequently, high injection of electrons from the ohmic contact takes place with a concentration much greater than the equilibrium concentration in the conduction band. In this case, the resistance modulation of the bulk (neutral) part of the CdTe crystal occurs [16,42]. This process is enhanced with increasing temperature. An agreement between the calculation results of the total reverse current $I = I_g + I_{SCLC}$ in the Mo-MoO_x/*p*-CdTe/MoO_x-Mo, Ti-TiO_x/*p*-CdTe/MoO_x-Mo, and Ti-TiN/*p*-CdTe/MoO_x-Mo heterostructures and experimental data was achieved for the trap level with the ionization energy $E_t = 0.6 \pm 0.02$ eV.

At higher bias voltages, the reverse *I-V* characteristics of the Schottky-diode detectors of Mo-MoO_x/*p*-CdTe/MoO_x-Mo (d) and Ti-TiN/*p*-CdTe/MoO_x-Mo (at $|V| > 125$ V) and Ti-TiO_x/*p*-CdTe/MoO_x-Mo (at $|V| > 90$ V) become the power-law voltage dependence of the current $I \sim V^{3.6}$ (Figure 4a,d and c, respectively). According to the SCLC theory, it can be explained as the trap-filling limit [47,48]. The standard SCLC theory assumes that the potential barrier height E_t of the trap in Equation (5) is constant for any value of the applied electric field. However, the activation energy of the reverse current at high voltages (when $I \sim V^{3.6}$) is lower (0.25-0.5 eV) (Figure 4). It is quite reasonably assumed that the barrier height of the trap lowered at high electric fields and this is due to the Poole–Frenkel electron emission from the oxide layer [49,50]. This charge transport mechanism is usually used to explain the electrical characteristic features of the metal-insulator-semiconductor structures [46,51]. Such assumption is realistic in view of the probable formation of thin Cd-rich or Te-rich surface layers under the preliminary surface chemical processing of CdTe single-crystal wafers [52,53]. Indeed, polishing chemical etching of the CdTe samples in a $K_2Cr_2O_7 + HNO_3 + H_2O$ solution before electrodes deposition results in enriching the semiconductor surface with excess Cd or Te promotes the formation of oxides and other surface inhomogeneities [52].

According to the Poole-Frenkel model, the conductivity of the insulating film in the metal–insulator–semiconductor structure is due to thermal excitation of electrons from trapping centers located in the bandgap of the insulator (Figure 6a). Therefore, the temperature dependence of the conductivity is described by the factor $\exp(-E_t/kT)$, where E_t is the trapping level energy (trap ionization energy at zero electric field) [50,51]. Even if the applied bias voltage is moderate, the electric field in a thin insulating film is quite high. Therefore, the potential barrier height for electrons at the trapping center decreases and thermal excitation of electrons can be sufficiently enhanced. According to the Poole-Frenkel emission model, in the case of Coulomb potential states of the trap in the insulator with the thickness d_i, the current can be expressed as [50,51]

$$I_{PF} = Aq\mu_n \frac{V}{d_i} N_c \exp\left(-\frac{E_t}{kT}\right) \exp\left(-\frac{q\sqrt{qV/\pi\varepsilon\varepsilon_0 d_i}}{kT}\right), \quad (6)$$

where the last factor takes into account the barrier lowering induced by the electric-field due to the Poole–Frenkel effect. The square-root voltage dependence in the exponent for this factor is a feature of Poole-Frenkel emission [51]. As seen, the experimental data on the voltage dependence of the current presented in the corresponding coordinates are linear (Figure 6b).

Preprints (www.preprints.org) | NOT PEER-REVIEWED | Posted: 2 April 2021 doi:10.20944/preprints202104.0079.v1

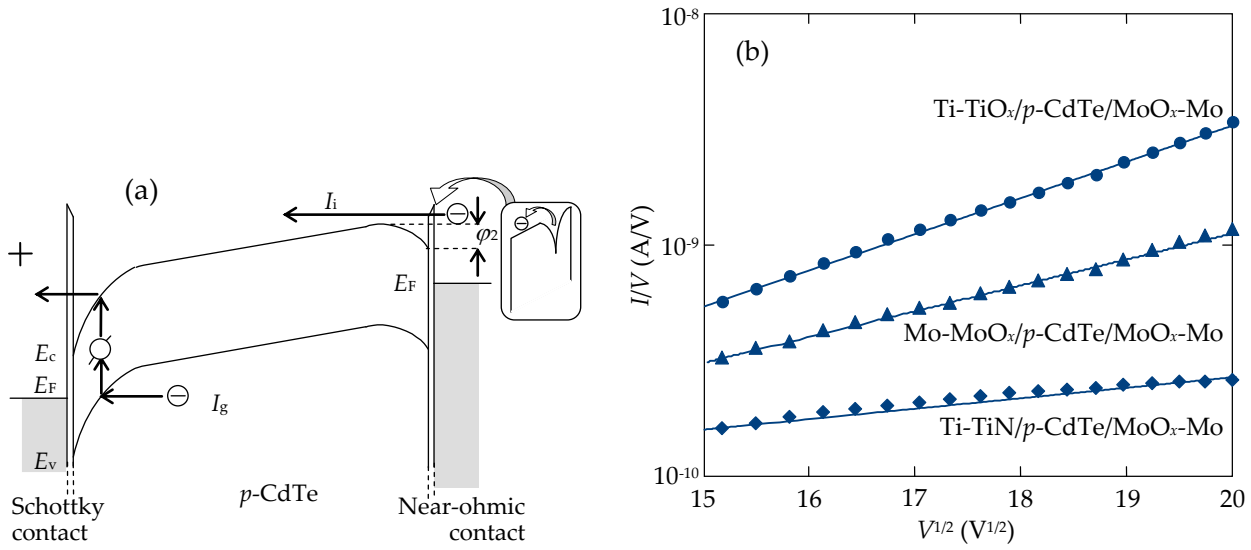

Figure 6. (**a**) Illustration of the Poole-Frenkel emission from the near-ohmic contact (CdTe/MoO$_x$) showing the injection I_i and generation I_g currents (arrows) in the energy diagram of the reverse-biased CdTe-based heterostructure (the Schottky contact is biased positively with respect to the near-ohmic one). (**b**) Comparison of the results calculated according to the Poole-Frenkel emission model by Equation (6) (solid lines) with the measured *I–V* characteristics of the reverse-biased Mo-MoO$_x$/*p*-CdTe/MoO$_x$-Mo, Ti-TiO$_x$/*p*-CdTe/MoO$_x$-Mo, and Ti-TiN/*p*-CdTe/MoO$_x$-Mo Schottky-diode detectors (symbols).

This confirms the assumption about the nature of excess charge carriers. Thus, the Poole-Frenkel emission of electrons from the CdTe/MoO$_x$ near-ohmic contact to the semiconductor explains the increased electrical conductivity and the region with the dependence $I \sim V^{3.6}$ in the *I–V* characteristics of the reverse-biased Mo-MoO$_x$/*p*-CdTe/MoO$_x$-Mo, Ti-TiO$_x$/*p*-CdTe/MoO$_x$-Mo, and Ti-TiN/*p*-CdTe/MoO$_x$-Mo heterostructures at higher applied bias voltages (Figure 4a,c,d).

In terms of using the X/γ-ray detectors under study as spectroscopic instruments, it is useful to note that the *I-V* characteristic of the Ti-TiN/*p*-CdTe/MoO$_x$-Mo detector is linear in the voltage range 15 V < *V* < 110 V (Figure 4d). Such a behavior of the *I-V* characteristic is explained by the circumstance that the depleted region in the Ti-TiN/*p*-CdTe/MoO$_x$-Mo Schottky diode occupies almost the entire thickness of the semiconductor crystal, i.e. this region is limited by the crystal thickness. The bias voltage required to achieve such condition is called the depletion voltage [48]. This value can be found from Equation (4) as $V_d = qNd^2/2\varepsilon\varepsilon_0$. Assuming the CdTe crystal thickness d = 0.5 mm and uncompensated acceptor concentration $N = 5 \times 10^{10}$ cm^{-3}, the depletion voltage is V_d = 10.6 V. With higher applied bias voltage, a more uniform electric field profile is across the entire semiconductor wafer thickness can be achieved. The CdTe crystal behaves as a sample with a resistivity higher than that of the bulk (neutral) part of the semiconductor. Such regime of charge transport results in a linear voltage dependence of the current that is observed as $I \sim V^1$ (Figure 4d). As shown below (section 5), the bias voltages range 15 V< *V* < 110 V is the most promising for employing Ti-TiN/*p*-CdTe/MoO$_x$-Mo detectors as spectroscopic instruments.

4. Capabilities of CdTe-based X/γ-Ray Detectors with an In Contact Treated by Laser Pulse Radiation

4.1. Laser-assisted formation of In/CdTe/Au diode structures

4.2.1. Techniques of CdTe Crystal Surface processing and Electrical Contact Formation

Before electrical contact formation and electrode deposition, detector-grade (111) oriented CdTe single-crystal wafers were preliminarily subjected to chemical surface processing for cleaning and removing of a disordered surface layer which was generally

Preprints (www.preprints.org) | NOT PEER-REVIEWED | Posted: 2 April 2021 doi:10.20944/preprints202104.0079.v1

formed after mechanical polishing and storage of semiconductor crystals [52,53]. The CdTe samples were cleaned in acetone and methanol, then etched in a polishing 3-5% bromine-methanol solution, and finally were thoroughly rinsed with pure methanol. The polished and cleaned samples were dried in an argon flow before applying the next technological procedures of electrical contact formation and laser-induced doping.

The techniques of the fabrication of the In/CdTe/Au diodes with a *p-n* junction are shown in Figure 7. After the preliminary surface processing, the CdTe crystals were subjected to low temperature (~70-90 °C) annealing in a vacuum chamber at low pressure (< 0.6 mPa) during 1.5-2 hours before the metal contact deposition to remove a thin (~ 0.03 nm) Te film which was generally formed on the semiconductor surface under etching in bromine-containing solutions and then oxidized [52,53]. Then, an In film was evaporated on the CdTe(111)*B* crystal surface without heating of the samples (Figure 7a). The whole surface area of the CdTe crystal pre-coated with an In film was entirely and uniformly irradiated with nanosecond laser pulses at room temperature (Figure 7b). It was shown that distilled water environment was the optimal ambient condition for such treatment [54]. A KrF excimer laser, emitting single pulses with a wavelength of 248 nm and duration of 20 ns, was a pulsed radiation source. The incident laser pulse energy density was varied in wide ranges both below and above the CdTe melting threshold [27]. A glass diffuser, homogenizer, and lens were used to provide uniform and controlled laser irradiation of the In/CdTe samples. The time and energy parameters of laser pulses were monitored under irradiation. The deposited In film was relatively thick (0.3-0.5 μm) and it was not completely evaporated at laser irradiation, thus the film served both as an *n*-type dopant source and electrical contact (electrode) after laser-induced doping (Figure 7c).

The second electrode was formed on the opposite side of the samples, i.e. on the CdTe(111)*A* surface by vacuum thermal evaporation of an Au film (0.3-0.5 μm) (Figure 7d). Both the In and Au electrodes were formed as 4 × 4 mm^2 squares and centered on the Te- and Cd-terminated surfaces (5 × 5 mm^2) of the sample, respectively. The deposition velocity and thickness of the electrodes (In and Au films) were controlled by the voltage applied to the evaporating metal source and monitored with an XTC thin film deposition controller. After laser irradiation of the In/CdTe structure from the In-coated side and prior to the Au electrode deposition, the sample was subjected to chemical passivation in an aqueous H_2O_2 solution, and then was rinsed in methanol (Figure 7d). Such procedure was employed to minimize lateral leakage currents, create the appropriate surface states at the CdTe(111)*A* side, and stabilize electrical characteristics of the In/CdTe/Au diode structures.

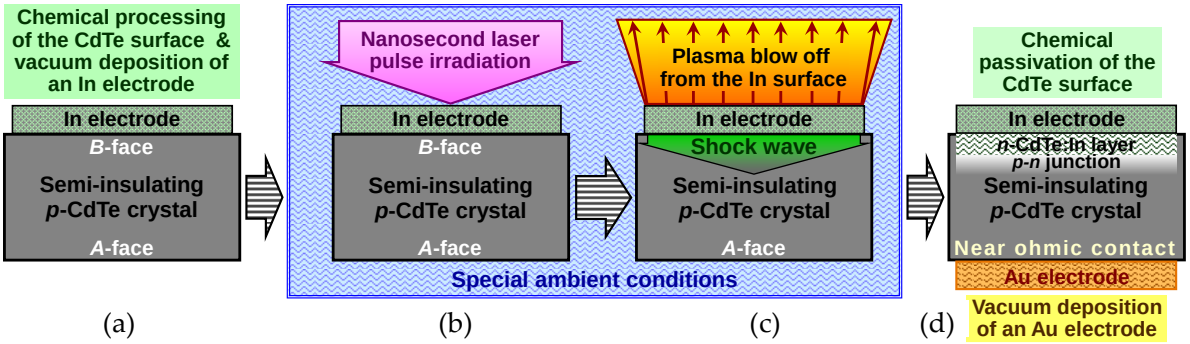

Figure 7. Schematic illustration of the fabrication procedures of In/CdTe/Au diode detectors using the laser irradiation technique: (**a**) chemical surface processing of the crystal and thermal vacuum deposition of an In electrode (dopant film) on the CdTe(111)*B* surface; (**b**) irradiation of the In/CdTe structure with nanosecond laser pulses; (**c**) laser-induced shock wave solid-phase doping of the *p*-CdTe surface region by In atoms (donors) and formation of a *p-n* junction; (**d**) chemical passivation of the crystal surfaces and thermal vacuum deposition of an Au electrode on the CdTe(111)*A* surface.

4.2.2. Mechanisms of laser action on the In/CdTe structure and *p-n* junction formation

Preprints (www.preprints.org) | NOT PEER-REVIEWED | Posted: 2 April 2021 doi:10.20944/preprints202104.0079.v1

The use of a relatively thick In electrode (0.3 0.5 μm) which also served as an dopant film, made it possible to ensure laser-induced doping without heating the underlying bulk In region and CdTe crystal that avoided a heat-induced deterioration of the structure and properties of the semiconductor. Despite the fact that absorption of laser radiation occurred in a thin (tens of nanometers) In surface layer, high doping of the semiconductor with In atoms under the In/CdTe interface region was occurred [54,55]. It was supposed that In/CdTe/Au diode structures with an In doped CdTe nano-layer and built-in *p-n* junction were obtained as a result of laser-stimulated modification of the defect structure and solid-phase doping in the deep-seated CdTe region.

Figure 7c illustrates the laser pulse action on the In/CdTe structure that was accompanied with superfast heating, melting, and evaporation of a thin (in order of the radiation absorption depth) In surface layer. The temperature of the laser-induced plasma (evaporated In and overheated environment medium, i.e. water), could reach 1000 °C and higher at laser pulse energy densities used in the experiment (80-130 mJ/cm^2). Rapid expansion of the laser-heated In surface region and plasma recoil momentum resulted in generation of high-amplitude stress waves which could be transformed to a high pressure shock wave [56]. Laser-induced stress and shock waves propagated through the In film and entered into the CdTe crystal involving In dopant atoms [54,55]. Laser-stimulated penetration of high concentration In dopant into the thin semiconductor region near the In-CdTe interface was caused by essential elastic stress gradients, generation of stress and shock waves, and superfast diffusion of In atoms due to barodiffusion [55]. Despite high temperatures of the In electrode surface under laser irradiation, underlying deeper layers remained almost unheated because the deposited In film was much thicker than the laser-heated In surface region, therefore the temperature in the bulk of In and particularly in CdTe was not significantly increased. This provided the optimal conditions for solid-phase doping of a thin CdTe layer owing to rapid mass transfer of the In impurity and transformation of the semiconductor point defect structure near the In/CdTe interface as a result of shock wave action and barodiffusion [55].

The fabricated In/CdTe/Au diode detectors were considered as complex metal-semiconductor multi-layered structures consisting of the following: In electrode, In/*n*-CdTe ohmic contact, low-resistivity highly doped *n*-CdTe:In layer, abrupt *p-n* junction, bulk part of semi-insulating *p*-CdTe, Au/*p*-CdTe near ohmic contact and Au electrode (Figure 7d). Laser-induced doping of semi-insulating Cl-compensated *p*-like CdTe crystals was due to the transformation of the semiconductor point defect structure [27,54]. Detector-grade high-resistivity CdTe:Cl semiconductor contains a large number of intrinsic and impurity point defects, in particular, V_{Cd} and Cl_i, Cl_{Te} or other substitutional impurities in a Te site [3-7]. The point defects are generally aggregated as complexes (V_{Cd}-Cl_{Te}), (V_{Cd}-2Cl_{Te}) or (V_{Cd}-Cl_i) [6,7]. In detector grade CdTe:Cl or CdTe:In crystals, typical complex acceptor defects, called A-centers ((V_{Cd}-Cl_{Te}) and (V_{Cd}-In_{Cd})), are formed that results in *p*-type conductivity of the semiconductors and moreover, spontaneous formation of compensating acceptors (V_{Cd}-In_{Cd}) is the general problem in *n*-type doping of CdTe with an In impurity [6,57].

The main advantage of the modification of the CdTe structure and properties under laser irradiation of the crystals pre-coated with a relatively thick In film, was the action of an induced shock wave that could be considered as a stream of phonons scattered by point and extended defects of the CdTe structure. Such action resulted in the dissociation of defect complexes, barodiffusion of an In dopant atoms, desorption and segregation of interstitial atoms [27,54-56]. In the case of nanosecond laser irradiation of the In/CdTe structures, In dopant atoms implicated by laser-induced stress and shock waves penetrated into the CdTe region near the metal-semiconductor interface [27,54]. Laser stimulated processes of barodiffusion and migration of In atoms at V_{Cd} and then super-fast "freezing" of a large number of donor point defects as In_{Cd}, Cd_i and Cl_{Cd} without formation of compensating acceptor complexes (V_{Cd}–X), in particular A-centers like (V_{Cd}–

Preprints (www.preprints.org) | NOT PEER-REVIEWED | Posted: 2 April 2021 doi:10.20944/preprints202104.0079.v1

Cl_{Te}) and (V_{Cd}–In_{Cd}), ensured solid-phase high In doping of a thin CdTe layer near the In/CdTe interface and formation of an abrupt *p-n* junction [27,54,55].

4.2. Electrical Characteristics of In/CdTeAu Diode Structures Fabricated by Laser Irradiation

Semiconductor diode-type ionizing radiation detectors operate in reverse bias mode and respond to incident X/γ-ray photons [4-8]. Therefore, it is important to obtain low reverse dark current (leakage current) in diode detectors. This allows applying higher reverse bias voltages to extend the depletion region up to the whole thickness of a semiconductor crystal and thus achieve better or even full collection of photogenerated charge carriers and hence obtain higher energy resolution [4-8, 16-18, 33].

The In/CdTe/Au diode structures with a *p-n* junction, formed by laser irradiation of the In electrode, were exanimated by electrical measurements and samples with low reverse dark currents were selected for testing them as X/γ-ray radiation detectors. Reverse current flowed when the In contact (near the *p-n* junction) was biased positively with respect to the Au contact (quasi-ohmic). Figure 8 shows the typical *I-V* characteristics of the In/CdTe/Au samples fabricated without laser irradiation of the In electrode (a) and with irradiation by nanosecond pulses of a KrF excimer laser with energy densities of ~ 90 J/cm² (b) and ~110 J/cm² (c). The *I-V* characteristics of the In/CdTe/Au diodes, measured in dark conditions at room temperature, showed excellent rectifying properties, especially taking into account the fact that CdTe crystals used for detector fabrication were semi-insulating (Figure 8).

In the case of unirradiated In/CdTe/Au samples with just deposited In and Au electrodes (Figure 8a), the rectification was due to a high Schottky barrier at the In/CdTe interface that was typical for an In electrical contact and semi-insulating *p*-like CdTe and this was widely used for fabrication of Schottky diode detectors [5-10]. Moreover, the rectification significantly increased after laser irradiation of the In/CdTe structure (Figure 8b,c). As discussed in the section above, it was resulted from laser-induced doping of the thin CdTe region under the In/CdTe interface with an In donor dopant and formation of a shallow and abrupt *p-n* junction according to the mechanisms investigated earlier [27,54,55]. As seen, laser irradiation of the In/CdTe structure from the In electrode side remarkably shifted the *I-V* characteristic forward branch toward lower voltages (forward current increased) and reduced reverse current compared with the unirradiated In/CdTe/Au sample (Figure 8b,c). From a practical point of view, it is important to note that the reverse current of the In/CdTe/Au *p-n* junction diodes reduced by more than 250 times due to laser treatment of the In electrode (Figure 8c).

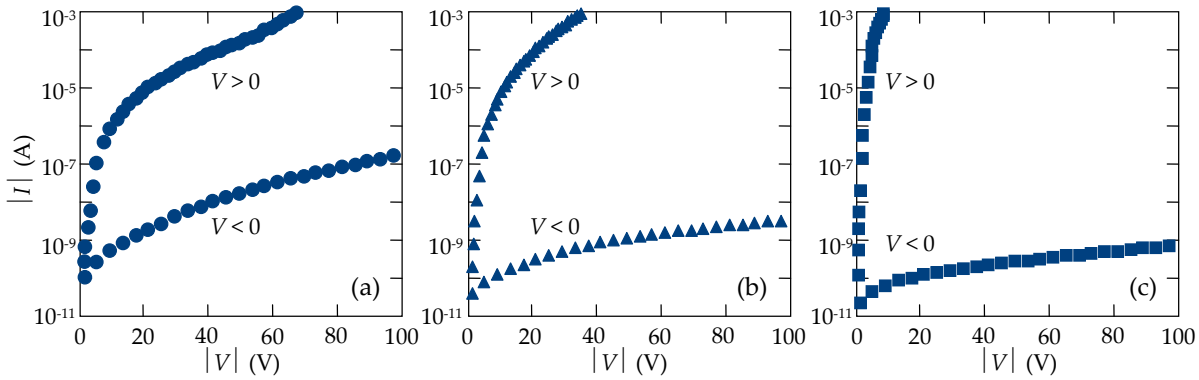

Figure 8. *I-V* characteristics of the In/CdTe/Au diode structures in double logarithmic coordinates (**a**) before and (**b**,**c**) after irradiation from the In electrode side by nanosecond pulses of a KrF excimer laser with the energy density of (**b**) 90 J/cm² and (**c**) 120 J/cm².

Figure 9 presents the comparison of the calculation results using Equations (1)-(4) (solid lines) and experimental results (symbols). It should be emphasized that the calculations were performed at the concentration of uncompensated acceptors $N = N_a - N_d = 5 \times$

Preprints (www.preprints.org) | NOT PEER-REVIEWED | Posted: 2 April 2021 doi:10.20944/preprints202104.0079.v1

10^{10} cm^{-3} as it corresponded to CdTe single crystals produced by Acrorad [19-25] and the ionization energy of the generation–recombination center was accepted as E_t = 0.67 eV. The computed results exhibited that the lifetimes τ_{n0} of electrons and holes τ_{p0} were such critical parameters determining the reverse current values in the *I-V* characteristics.

As mentioned in the section above, the laser-generated stress and shock waves penetrated into the semiconductor region near the In/CdTe interface implicating In atoms and introducing them as a dopant into the crystal lattice that decreased the concentration of vacancies in that region. In particular, Cd vacancies were partly filled by the nearest accidental impurities, mainly by In dopant atoms [27,54]. In atoms, substituting Cd atoms, acted as donors [6,57]. So, the impact of laser irradiation increased the effective lifetimes of charge carriers in the depleted layer, reduced the generation rate, and thus decreased the reverse dark current of In/CdTe/Au *p-n* junction detectors.

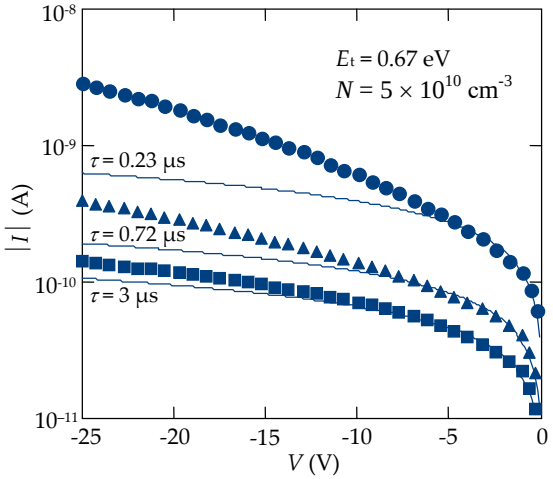

Figure 9. Comparison of the experimental (symbols) and calculated according to the Sah-Noyce-Shockley theory (solid lines) results of the reverse dark *I-V* characteristics of the In/CdTe/Au diode structures before (circles) and after (squares and triangles) irradiation from the In electrode side by nanosecond pulses of a KrF excimer laser with the energy density of 90 J/cm^2 (triangles) and 120 J/cm^2 (squares).

As seen from Figure 9, the Sah-Noyce-Shockley theory describes well the reverse dark current in the unirradiated In/CdTe/Au diode only in the voltage range $0 < |V| < 5$ V (circles). The sections of the plots where the experimental results coincide with calculations expand in In/CdTe/Au diode structures formed by laser irradiation. In particular, the generation current prevails in the In/CdTe/Au diode after laser treatment with the energy density of 90 J/cm^2 in the voltage range $0 < |V| < 10$ V (triangles), whereas the laser irradiation with the energy density of 120 J/cm^2 leads to the increasing the voltage range, corresponding to the generation current, up to ~15 V (squares).

5. Spectroscopic Characteristics of CdTe-Based X/γ-Ray Detectors

The spectroscopic performance including the energy resolutions of the fabricated CdTe-based detectors was examined using ^{241}Am (59.5 keV), ^{57}Co (122 keV), and ^{137}Cs (662 keV) isotopes as X/γ-ray radiation sources as well as employing a portable spectrometer ANS-MNT004-GTK produced by ANSeeN, Inc. or standard laboratory equipment (a charge-sensitive preamplifier 5102 BS produced by Clear Pulse Co., Ltd., coupled to a multichannel analyzer MCA7600 produced by Seiko EG&G Co., Ltd., etc.) in the case of investigation of the In/CdTeAu *p-n* junction diode detectors. The spectroscopic measurements were carried out at room temperature. The electrodes deposited on the CdTe(111)*A* surface (Cd-terminated) were biased negatively for all the tested detectors.

The energy resolution of the developed detectors was determined by the fabrication techniques and materials chosen for electrical contact formation as well as was depended

Preprints (www.preprints.org) | NOT PEER-REVIEWED | Posted: 2 April 2021 doi:10.20944/preprints202104.0079.v1

on the applied bias voltage. The voltage dependences of the energy resolution (FWHM) slightly differed for CdTe-based detectors created by the same techniques but under different conditions. It can be explained by the decreasing of the misfit strains at the interface between the thin contact film and bulk crystal. In particular, for the Mo-MoO_x/*p*-CdTe/MoO_x-Mo, Ti-TiO_x/*p*-CdTe/MoO_x-Mo, Ti-TiN/*p*-CdTe/MoO_x-Mo, and In/*p*-CdTe/MoO_x-Mo structures the misfit strain was determined by well-known ratio [58] and equals to 14%, 29%, 34%, and 18%, respectively. Another reason for differences in the energy resolutions could be due to different surface states at the CdTe crystal surfaces when electrical contacts were deposited [20-24]. There were the optimal bias voltages for each detector with MoO_x contacts at which the energy resolution and detection efficiency reached the best values.

In Table 1, the energy resolution values for the 59.5 keV and 662 keV peaks in the spectra of ^{241}Am and ^{137}Cs isotopes are respectively presented for the detectors with different contact materials at different combinations of applied bias voltages. For the CdTe-based structures with the same electrical contacts, the energy resolutions varied from the detector to detector by ~25%. At lower bias voltages, the energy resolution worsened due to insufficient field strength to collect photogenerated charge carriers and at higher voltages, deterioration in the energy resolution was due to excessive dark current in the detectors. Some of the reasons for such features of the detectors were the effect of the CdTe crystal defect structure and misfit strains in the transition layer at the electrical contact-bulk semiconductor interface. Here the results for the best performance of the detectors with one MoO_x contact and the second one made from different materials are presented.

Table 1. Energy resolutions of the CdTe-based detectors with different contact materials, measured at different bias voltages for two X/γ-ray radiation sources.

X/γ-ray source	Anode/CdTe/Cathode	Bias voltage (V)	FWHM (%)
^{241}Am (59.5 keV)	Mo-MoO_x/*p*-CdTe/MoO_x-Mo	80	6
	Ti-TiO_x/*p*-CdTe/MoO_x-Mo	100	> 20
	Ti-TiN/*p*-CdTe/MoO_x-Mo	80	11
	In/*p*-CdTe/MoO_x-Mo	100	> 25
^{137}Cs (662 keV)	Mo-MoO_x/*p*-CdTe/MoO_x-Mo	100	7.9
	Ti-TiO_x/*p*-CdTe/MoO_x-Mo	100	9
	Ti-TiN/*p*-CdTe/MoO_x-Mo	100	10.1
	In/*p*-CdTe/MoO_x-Mo	120	5.1

The energy resolution of the detectors strongly depended on the applied bias voltage (Figures 10 and 11). The spectra with the best FWHM values at the corresponding voltages are presented in Figure 10. The highest resolution was obtained for the In/*p*-CdTe/MoO_x-Mo detector and it was reached at V = 120 V, i.e. the lowest value of FWHM = 5.1% (Figure 10b). However, FWHM rose rapidly with increasing bias voltage due to a sharp increase in the dark current of the detector (Figure 4b).

Preprints (www.preprints.org) | NOT PEER-REVIEWED | Posted: 2 April 2021 doi:10.20944/preprints202104.0079.v1

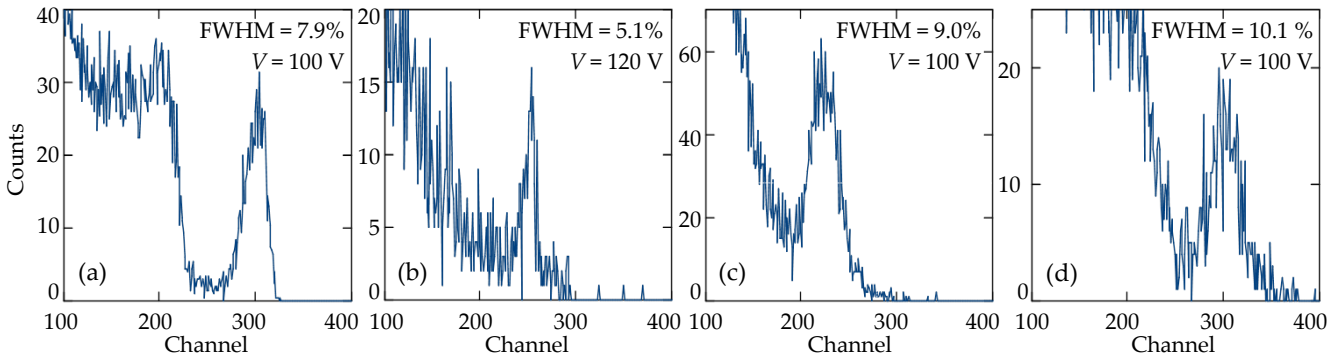

Figure 10. Room temperature spectra of a ^{137}Cs (662 keV) isotope taken with the (**a**) Mo-MoO$_x$/*p*-CdTe/MoO*x*-Mo, (**b**) In/CdTe/MoO$_x$-Mo, (**c**) Ti-TiO$_x$/*p*-CdTe/MoO$_x$-Mo, and (**d**) Ti-TiN/*p*-CdTe/MoO$_x$-Mo detectors.

The development techniques of modification of the surface state of semi-insulating *p*-like CdTe crystals and electrical contact formation using nanosecond pulse laser irradiation resulted in the optimization of the detector fabrication technology that made it possible to obtain In/CdTe/Au diode-type X/γ-ray sensors with higher detection efficiency and energy resolution in comparison with the Mo-MoO$_x$/*p*-CdTe/MoO$_x$-Mo, In/CdTe/MoO$_x$-Mo, Ti-TiO$_x$/*p*-CdTe/MoO$_x$-Mo, and Ti-TiN/*p*-CdTe/MoO$_x$-Mo detectors which we also elaborated, fabricated and investigated. However, CdTe-based detectors with molybdenum oxide ohmic contacts and titanium oxide, titanium nitride, and indium Schottky contacts have shown promise and it is possible to achieve better performance by modification and optimization of the technology procedures of CdTe crystal surface preparation and electrode deposition techniques using different contact materials [20-24,34-39].

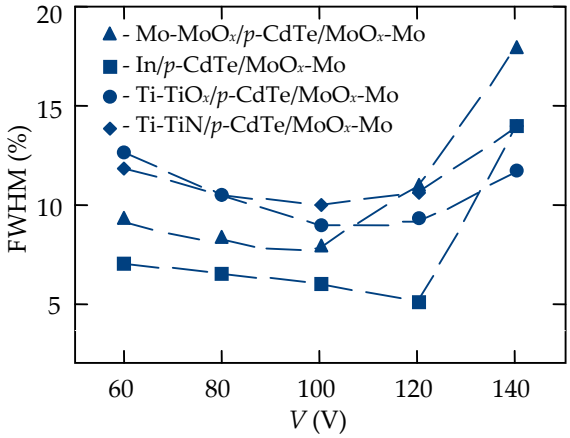

Figure 11. Effect of the bias voltage applied to the Mo-MoO$_x$/*p*-CdTe/MoO$_x$-Mo (triangles), In/CdTe/MoO$_x$-Mo (squares), Ti-TiO$_x$/*p*-CdTe/MoO$_x$-Mo (circles), and Ti-TiN/*p*-CdTe/MoO$_x$-Mo (diamonds) detectors on the energy resolution (FWHM) of the 662 keV photopeak in the room temperature ^{137}Cs isotope spectra.

Due to creating the appropriate conditions for photogenerated charge carrier collection, lowering the reverse dark (leakage) current in the In/CdTe/Au *p-n* junction diode detectors and thus increasing detecting ability and decreasing electrical noises in the detectors, the spectra of ^{241}Am ^{57}Co, and ^{137}Cs isotopes with quite high energy resolutions were obtained (Figure 12). There was also found a certain optimal bias voltage range for each In/CdTe/Au *p-n* junction detector that provided a higher number of counts (better detection efficiency), lower FWHM values for the isotope spectrum photopeaks (higher energy resolution), and true peak channel positions (Figure 12).

Preprints (www.preprints.org) | NOT PEER-REVIEWED | Posted: 2 April 2021 doi:10.20944/preprints202104.0079.v1

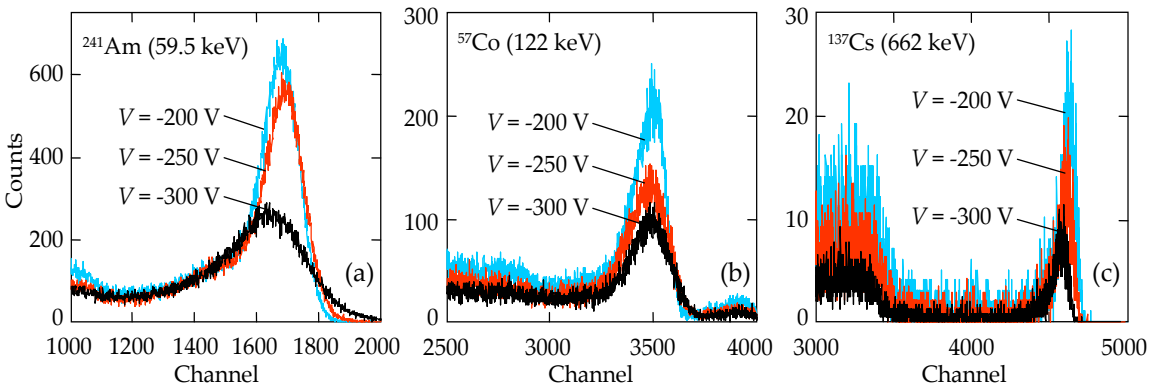

Figure 12. Room temperature spectra of (**a**) ^{241}Am (59.5 keV), (**b**) ^{57}Co (122 keV), and (**c**) ^{137}Cs (662 keV) isotopes at different bias voltages (200 V, 250 V, and 300 V) taken with the In/CdTe/Au *p-n* junction detector, fabricated by laser radiation of the In electrode.

Table 2 presents the data on the energy resolutions of the In/CdTe/Au *p-n* detector calculated for the emission spectra of three isotopes measured at different bias voltages (Figure 12). As seen, the best FWHM values were obtained in the spectra taken at V = -200 V. The quite symmetric shape of the prominent lines of 59.5 keV, 122 keV and 662 keV in the spectra of ^{241}Am, ^{122}Co and ^{137}Cs isotopes, respectively, for all the applied bias voltages evidences that the full charge collection was complete even at the lowest bias voltage V = 200 V (Figure 12). The broad shoulder at the low-energy side from the 662 keV line (c) was attributed to Compton scattering of γ-rays [7-10].

Table 2. Energy resolutions of the In/CdTe/Au *p-n* junction detector, fabricated by laser radiation of the In electrode, measured at different bias voltages for three X/γ-ray radiation sources.

X-ray source	Bias voltage (V)		
	200	250	300
	FWHM (%)		
^{241}Am (59.5 kev)	7.5	9.04	14.72
^{57}Co (122 keV)	4.79	5.62	6.19
^{137}Cs (662 keV)	1.6	2.1	2.7

An increase in bias voltage (V = 250 V and V = 300 V) resulted in deterioration of the spectra: the number of counts decreased (Figure 12a,b,c), the FWHM values increased (Figure 12a,b,c) and the peak channel positions for the 59.5 keV (a) and 662 keV (c) lines were shifted toward the lower-energy side (Figure 12). Such distortion in the isotope spectra with rising bias voltages was attributed to an increase in the total reverse current, i.e. photocurrent (charge packet) and leakage current (mainly due to lateral currents because no any guard ring was used in the experiments).

The features of the CdTe-based X/γ-ray detectors with different contact materials were studied in details earlier [17-33]. The capabilities of the developed detectors to operate for long time without deterioration of their functional parameters were shown and analyzed. However, further improvement of spectroscopic properties of CdTe-based detectors can be achieved by the optimal choice of contact materials, pre-treatment procedures of the semiconductor crystal surfaces, and corresponding techniques of electrode deposition.

6. Conclusions

Based on the developed efficient techniques of semiconductor crystal surface processing and electrode deposition, X/γ-ray detectors with different contact materials were fabricated using the same detector-grade *p*-like CdTe produced by Acrorad Co. The heterostructures with ohmic (MoO_x) and Schottky (MoO_x, TiO_x, TiN, and In) contacts, cre-

ated by DC reactive magnetron sputtering and vacuum thermal evaporation, were characterized by electrical and spectroscopic measurements. It was shown the possibility of application of molybdenum oxide thin films both as an ohmic or Schottky contact to semi-insulating *p*-CdTe crystals depending on pre-treatment of their surfaces. The fabricated Mo-MoO_x/*p*-CdTe/MoO_x-Mo, In/CdTe/MoO_x-Mo, Ti-TiO_x/*p*-CdTe/MoO_x-Mo, and Ti-TiN/*p*-CdTe/MoO_x-Mo Schottky-diode detectors showed high rectification properties with quite low reverse dark currents and were sensitive to X/γ-ray radiation with moderate energy resolutions (5-20%@59.5 keV, 5-10%@662 keV). Comparison of the *I-V* characteristics of the investigated Schottky-diode heterostructures and well-known theoretical models allowed us to explain the mechanisms of charge carrier transport and clarify the reasons limiting the energy resolution of the fabricated heterostructures as X/γ-ray detectors. The charge transport mechanisms, dominating in the heterostructures at certain bias voltage ranges, were attributed to the generation-recombination in the SCR at low bias voltages, SCLC at higher voltages, and Poole-Frenkel emission at highest applied biases. The last effect limited the use of the developed Schottky diode heterostructures as X/γ-ray detectors at high bias voltages.

Higher energy resolutions (7-15%@59.5 keV, 4-6%@122 keV, and 1.6-3%@662 keV) were obtained by the developed In/CdTe/Au diode detectors with a *p-n* junction formed by laser-induced doping of a thin CdTe surface layer with In atoms (donors). This was realized by irradiation of the *p*-CdTe crystals pre-coated with an In dopant film with nanosecond laser pulses. The analysis of the *I-V* characteristics of the In/CdTe/Au structures evidenced that laser irradiation of the In electrode increased the bias voltage range corresponding to the charge transport mechanism of the carrier generation-recombination in the SCR.

The use of different contact materials along with modification and optimization of the techniques of surface processing of semiconductor crystals, contact formation, and electrode deposition expand the possibilities to achieve better performance of room temperature CdTe-based X/γ-ray detectors.

Author Contributions: Conceptualization, O.M. and V.G.; methodology, O.M. and V.G.; software, O.M. and V.G.; validation, M.S., V.B and T.A.; formal analysis, O.M. and V.G.; investigation, O.M., M.S., and V.G.; resources, O.M., V.B., M.S., and V.G.; data curation, T.A. and M.S.; writing—original draft preparation, O.M.; writing—review and editing, V.G.; visualization, O.M. and V.G.; supervision, O.M., V.G., and T.A.; project administration, O.M., V.G., and T.A.; funding acquisition, T.A. All authors have read and agreed to the published version of the manuscript.

Acknowledgments: We thank Dr. E. Maistruk for *I-V* characteristic measurements of the detectors with MoO_x contacts. A part (V.G.) of the research is based on the 2021 Cooperative Research Project (Grant No 2016) of Research Center for Biomedical Engineering, Japan.

Conflicts of Interest: The authors declare no conflict of interest.

References

1. Cooper, P.N. *Introduction to Nuclear Radiation Detectors*, Reissue ed.; Cambridge University Press: Cambridge, UK, 2011; pp. 1-152.
2. Owens, A. Present detection systems (Chapter 6). In: *Compound Semiconductor Radiation Detectors*; Series in Sensors; CRC Press, Taylor & Francis: New York, USA, 2012; pp. 287- 368.
3. Zanio, K. Cadmium Telluride, In: *Semiconductors and Semimetals*, Academic Press: New York, USA, 1978; Volume 13, 235 p.
4. Zappettini, A. Cadmium telluride and cadmium zinc telluride (Chapter 8). In: *Single Crystals of Electronic Materials. Growth and Properties*, Woodhead Publishing: Cambridge, UK, 2019; pp. 273-301.
5. Hage-Ali, M.; Siffert, P. CdTe Nuclear Detectors and Applications. In: *Semiconductors for Room Temperature Nuclear Detector Applications*; Schlesinger T.E., James R.B., Eds.; Academic Press: San Diego, CA, USA, 1995; Volume 43, pp. 291–334.
6. Triboulet, R,; Siffert, P. *CdTe and Related Compounds; Physics, Defects, Hetero- and Nano-structures, Crystal Growth, Surfaces and Applications, Part II: Crystal Growth, Surfaces and Applications*, 1st ed., Elsevier: Amsterdam, 2010.
7. Del Sordo, S.; Abbene, L.; Caroli, E.; Mancini, A.M.; Zappettini, A.; Ubertini, P. Progress in the development of CdTe and CdZnTe semiconductor radiation detectors for astrophysical and medical applications. *Sensors* **2009**, *9*, 3491-3526.
8. Takahashi, T.; Watanabe, S.; Ishikawa, S. High-resolution CdTe detectors and application to gamma-ray imaging. In: *Semiconductor Radiation Detection Systems*, Taylor & Francis Group: New York, 2010, pp. 171-193.

9. Shiraki, H.; Funaki, M.; Ando, Y.; Tachibana, A.; Kominami, S.; Ohno, R. THM growth and characterization of 100 mm diameter CdTe single crystals. *IEEE Trans. Nucl. Sci.* **2009**, *56*, 1717-1723.
10. Shiraki, H.; Funaki, M.; Ando, Y.; Kominami, S.; Amemiya, K.; Ohno, R. Improvement of the productivity in the THM growth of CdTe single crystal as nuclear radiation detector. *IEEE Trans. Nucl. Sci.* **2010,** *57*, 395-399.
11. Arkad'eva, E.N.; Matveev, O.A.; Ryvkin, S.M.; Rud', Yu.V. Possibility of using cadmium telluride for making n-p gamma detectors. *Sov. Phys. – Tech. Phys.* **1966,** *11*, 846-854.
12. Toyama, H.; Nishihira, A.; Yamazato, M.; Higa, A.; Maehama, T.; Ohno, R.; Toguchi, M. Formation of aluminum Schottky contact on plasma-treated cadmium telluride surface. *Japan. J. Appl. Phys.* **2004,** *43*, 6371-6375.
13. Principato, F.; Turturici, A.A.; Gallo, M.; Abbene, L. Polarization phenomena in Al/p-CdTe/Pt X-ray detectors. *Nucl. Instrum. Methods Phys. Res. A* **2013,** *730*, 141-145.
14. Kosyachenko, L.A.; Sklyarchuk, V.M.; Sklyarchuk, O.V.; Maslyanchuk, O.L. Band gap of CdTe and $Cd_{0.9}Zn_{0.1}Te$ crystals. *Semiconductors* **2011,** *45*, 1273–1280.
15. Kosyachenko, L.A.; Aoki, T.; Maslyanchuk, O.L.; Melnychyk, S.V.; Sklyarchuk, V.M.; Sklyarchuk, O.V. Features of conduction mechanism of semi-insulating CdTe single crystals. *Semiconductors* **2010,** *44*, 699-704.
16. Kosyachenko, L.A.; Sklyarchuk, V.M.; Sklyarchuk, O.F.; Maslyanchuk, O.L.; Gnatyuk, V.A.; Aoki, T. Higher voltage Ni/CdTe Schottky diodes with low leakage current. *IEEE Trans. Nucl. Sci.* **2009,** *56*, 1827–1834.
17. Kosyachenko, L.A.; Aoki, T.; Lambro**p**oulos, C.P.; Gnatyuk, V.A.; Sklyarchuk, V.M.; Maslyanchuk, O.L.; Grushko, E.V.; Sklyarchuk, O.F.; Koike, A. High energy resolution CdTe Schottky diode γ-ray detectors. *IEEE Trans. Nucl. Sci.* **2013**, *60*, 2845-2852.
18. Kosyachenko, L.A.; Aoki, T.; Lambro**p**oulos, C.P.; Gnatyuk, V.A.; Melnychuk, S.V.; Sklyarchuk, V.M.; Grushko, E.V.; Maslyanchuk, O.L.; Sklyarchuk, O.F. Optimal width of barrier region in X/γ-ray Schottky diode detectors based on CdTe and CdZnTe. *J. Appl.Phys.* **2013**, *113*, 054504, 1-9.
19. Maslyanchuk, O.L.; Aoki, T.; Sklyarchuk, V.M.; Melnychuk, S.V.; Kosyachenko, L.A.; Grushko, E.V. High-efficiency cadmium telluride detectors of X γ-radiation. *Ukr. J. Phys.* **2014**, *59*, 17-33.
20. Maslyanchuk, O.; Kulchynsky, V.; Solovan, M.; Gnatyuk, V.; Potiriadis, C.; Kaissas, I.; Brus, V. Diodes based on semi-insulating CdTe crystals with Mo/MoO_x contacts for X- and γ-ray detectors. *Phys. Stat. Sol. C* **2017**, *14*, 1600232, 1-4.
21. Maslyanchuk, O.L.; Solovan, M.M.; Brus, V.V.; Kulchynsky, V.V.; Maryanchuk, P.D.; Fodchuk, I.M.; Gnatyuk, V.A.; Aoki, T., Potiriadis, C.; Kaissas, Y. Capabilities of CdTe-based detectors with MoO_x contacts for detection of X/γ-ray radiation. *IEEE Trans. Nucl. Sci.* **2017**, *64*, 1168–1172.
22. Maslyanchuk, O.L.; Solovan, M.M.; Maistruk, E.V.; Brus, V.V.; Maryanchuk, P.D.; Gnatyuk, V.A.; Aoki, T. Prospects of In/CdTe X- and γ-ray detectors with MoO Ohmic contacts. *Proc. SPIE* **2018**, 10612V, 1-6.
23. Maslyanchuk, O.; Solovan, M.; Brus, V.; Maryanchuk, P.; Maistruk, E.; Fodchuk, I.; Gnatyuk, V.; Aoki, T., Lambropoulos, C.; Potiriadis, K. Performance comparison of X- and γ-ray CdTe detectors with MoO_x, TiO_x and TiN Schottky contacts. *IEEE Trans. Nucl. Sci.* **2018**, *65*, 1365–1370.
24. Brus, V.V.; Maslyanchuk, O.L.; Solovan, M.M.; Maryanchuk, P.D.; Fodchuk, I.M.; Gnatyuk, V.A.; Vakhnyak, N.D.; Melnychuk, S.V.; Aoki, T. Graphene/semi-insulating single crystal CdTe Schottky-type heterojunction X- and γ-ray radiation detectors. *Scientific Reports* **2019**, *9*, 1065, 1-8.
25. Maslyanchuk, O.; Solovan, M.; Brus, V.; Maryanchuk, P.; Maistruk, E.; Fodchuk, I.; Gnatyuk, V. Charge transport features of CdTe X- and γ-ray detectors with Ti and TiO_x Schottky contacts, *Nucl. Instrum. Methods Phys. Res. A* **2021**, *988*, 164920, 1-8.
26. Lambropoulos, C.P.; Aoki, T.; Crocco, J.; Dieguez, E.; Disch, C.; Fauler, A.; Fiederle, M.; Hatzistratis, D.S.; Gnatyuk, V.A.; Karafasoulis, K.; Kosyachenko, L.A.; Levytskyi, S.N.; Loukas, D.; Maslyanchuk, O.L.; Medvids, A.; Orphanoudakis, T.; Papadakis, I.; Papadimitriou, A.; Potiriadis, C.; Schulman, T.; Sklyarchuk, V.M.; Spartiotis, K.; Theodoratos, G.; Vlasenko, O.I.; Zachariadou, K.; Zervakis, M. The COCAE detector: an instrument for localization - identification of radioactive sources. *IEEE Trans. Nucl. Sci.* **2011**, *58*, 2363-2370.
27. Gnatyuk, V.A.; Aoki, T.; Hatanaka, Y. Mechanisms of laser-induced defect formation and In doping in CdTe crystals. *IEEE Trans. Nucl. Sci.* **2004**, *51*, 2466-2471.
28. Aoki, T.; Ishida, Y.; Sakashita, D.; Gnatyuk, V.A.; Nakamura, A.; Tomita, Y.; Hatanaka, Y.; Temmyo, J. Development of energy discriminated CdTe imaging detector for hard x-ray. *Proc. SPIE* **2004,** *5540*, 196-205.
29. Aoki, T.; Gnatyuk, V.A.; Nakamura, A.; Tomita, Y.; Hatanaka, Y.; Temmyo, J. Study of a CdTe high-energy radiation imaging device fabrication by excimer laser processing. *Phys. Stat. Sol. C* **2004,** *1*, 1050-1053.
30. Gnatyuk, V.A.; Aoki, T.; Hatanaka, Y.; Vlasenko, O.I. Defect formation in CdTe during laser-induced doping and application to the manufacturing nuclear radiation detectors. *Phys. Stat. Sol. C* **2006,** *3*, 1221-1224.
31. Gnatyuk, V.A.; Aoki, T.; Vlasenko, O.I.; Levytskyi, S.N.; Dauletmuratov, B.K.; Lambropoulos, C.P. Modification of the surface state and doping of CdTe and CdZnTe crystals by pulsed laser irradiation. *Appl. Surf. Sci.* **2009**, *255*, 9813-9816.
32. Aoki, T.; Gnatyuk, V.A.; Kosyachenko, L.A.; Maslyanchuk, O.L.; Grushko, E.V. Transport properties of CdTe X/γ-ray detectors with *p-n* junction. *IEEE Trans. Nucl. Sci.* **2011**, *58*, 354-358.
33. Gnatyuk, V.A.; Aoki, T.; Grushko, E.V.; Kosyachenko, L.A.; Vlasenko, O.I. High resolution CdTe X- and gamma-ray detectors with a laser-formed *p-n* junction. *Proc. SPIE* **2011**, *8142*, 81420B-1-7.
34. Paudel, N.R.; Xiao, C.; Yan, Y. CdS/CdTe thin-film solar cells with Cu-free transition metal oxide/Au back contacts. *Prog. Photovolt: Res. Appl.* **2015**, *23*, 437–442.

35. Lin, H.; Irfan, Xia, W.; Wu, H.N.; Gao, Y.; Tang, C.W. MoO_x back contact for CdS/CdTe thin film solar cells: Preparation, device characteristics, and stability. *Sol. Energy Mater. Sol. Cells* **2012**, *99*, 349.
36. Irfan, I.; Turinske, A.J.; Bao, Z.; Gao, Y. Work function recovery of air exposed molybdenum oxide thin films. *Appl. Phys. Lett.* **2012**, *101*, 093305, 1-4.
37. Zhu, J.; Yang, Y.; Gao, Y.; Qin, D.; Wu, H.; Hou, L.; Huang W. Enhancement of open-circuit voltage and the fill factor in CdTe nanocrystal solar cells by using interface materials. *Nanotechnology* **2014**, *25*, 365203, 1-6.
38. Xue, H.; Wu, R.; Xie, Y.; Tan, Q.; Qin, D.; Wu, H.; Huang, W. Recent progress on solution-processed CdTe nanocrystals solar cells. *Appl. Sci.* **2016**, *6*, 197, 1-15.
39. Liu, H.; Tian, Y.; Zhang, Y.; Gao, K.; Lu, K.; Wu, R.; Qin, D.; Wu, H.; Peng, Z.; Hou, L.; Huang, W. Solution processed CdTe/CdSe nanocrystal solar cells with more than 5.5% efficiency by using an inverted device structure. *J. Mater. Chem. C* **2015**, *3*, 4227-4234.
40. Sah, C.-T.; Noyce, R.N.; Shokley, W. Carrier generation and recombination in p-n junctions and p-n junction characteristics. *Proc. IRE* **1957**, *45*, 1228–1243.
41. Kosyachenko, L.A.; Maslyanchuk, O.L.; Gnatyuk, V.A.; Lambropoulos, C.; Rarenko, I.M.; Sklyarchuk, V.M.; Sklyarchuk, O.F.; Zakharuk, Z.I. Charge collection properties of a CdTe Schottky diode for x- and γ-rays detectors. *Semicond. Sci. Technol.* **2008**, *23*, 075024, 1-8.
42. Kosyachenko, L.A.; Maslyanchuk, O.L.; Sklyarchuk, V.M. Special features of charge transport in Schottky diodes based on semi-insulating CdTe. *Semiconductors* **2005**, *39*, 722–729.
43. Yu, J.; Xu, L.; Zhang, B.; Zha, G.; Jie, W. On the current transport mechanism in metal–semiconductor–metal structured CdZnTe radiation detectors. *Nucl. Instrum. Methods Phys. Res. A* **2020**, *957*, 163445.
44. Kosyachenko, L.A.; Sklyarchuk, V.M.; Sklyarchuk, O.F.; Gnatyuk, V.A. Features of generation-recombination processes in CdTe-based Schottky diodes. *Semicond. Sci. Technol.* **2007**, *22*, 911–918.
45. Kosyachenko, L.A.; Maslyanchuk, O.L Efficiency spectrum of a CdTe X- and γ-ray detector with a Schottky diode. *Phys. Stat. Sol. C.* **2005**, *2*, 1194-1199.
46. Sze, S.M.; Ng, K.K. *Physics of Semiconductor Devices*, 3rd ed., John Wiley & Sons: Hoboken, New Jersey, 2007.
47. Lampert, M.A.; Mark, P. *Current Injection in Solids*, Academic Press: New York and London, 1970.
48. Zoul, A.; Klier, E. Space charge limited currents in high resistivity CdTe crystals. *Czech. J. Phys. B* **1977**, *27*, 789-796.
49. Frenkel, J. The theory of electric breakdown of dielectrics and electronic semiconductors. *Tech. Phys. USSR* **1938,** *5*, 685-695.
50. Frenkel, J. On pre-breakdown phenomena in insulators and electronic semi-conductors. *Phys. Rev.* **1938**, *54*, 647-648.
51. Kosyachenko, L.A.; Yatskiv, R.; Yurtsenyuk, N.S.; Maslyanchuk, O.L.; Grym, J. Graphite/CdMnTe Schottky diodes and their electrical characteristics. *Semicond. Sci. Technol.* **2013**, *29*, 015006, 1-10.
52. Reese, M.O.; Perkins, C.L.; Burst, J.M.; Farrell, S.; Barnes, T.M.; Johnston, S.W.; Kuciauskas, D.; Gessert, T.A.; Metzger, W.K. Intrinsic surface passivation of CdTe. *J. Appl. Phys.* **2015**, *118*, 155305, 1-12.
53. Gnatyuk, D.V.; Poperenko, L.V.; Yurgelevych, I.V.; Dacenko, O.I.; Aoki, T. Characterization of functional layers of CdTe crystals subjected to different surface treatments. *IEEE Trans. Nucl. Sci.* **2015**, *62*, 428-432.
54. Gnatyuk, V.A.; Levytskyi, S.N.; Vlasenko, O.I.; Aoki, T. Laser-induced doping of CdTe crystals in different environments, *Advanced Materials Research*. **2011**, *222*, 32-35.
55. Veleshchuk, V.P.; Baidullaeva, A.; Vlasenko, A.I.; Gnatyuk, V.A.; Dauletmuratov, B.K.; Levitskii, S.N.; Lyashenko, O.V.; Aoki, T. Mass transfer of indium in the In-CdTe structure under nanosecond laser irradiation. *Physics of the Solid State* **2010**, *52*, 469-476.
56. Gnatyuk, V.A.; Vlasenko, A.I.; Mozol', P.O.; Gorodnychenko, O.S. Role of laser-induced stress and shock waves in modification of the photoconductivity of $Cd_xHg_{1-x}Te$ films. *Semicond. Sci. Technol.* **1998**, *13*, 1298-1303.
57. Fochuk, P; Panchuk, O.; Feychuk, P.; Shcherbak, L.; Savitskyi, A.; Parfenyuk, O.; Ilashchuk, M.; Hage-Ali, M.; Siffert, P. Indium dopant behaviour in CdTe single crystals. *Nucl. Instrum. Methods Phys. Res. A*. **2001**, *458*, 104-112.
58. Liaw, I.-R.; Chol, K.-S.; Chang, S.-L. X-Ray double-crystal diffraction studies of CdTe/GaAs heteroepitaxjal layers. *J. Cryst. Growth* **1990**, *100*, 508-514.